

# SWCNT-SA mode-locked Tm:LuYO<sub>3</sub> ceramic laser delivering 8-optical-cycle pulses at 2.05 μm

YONGGUANG ZHAO,<sup>1</sup> LI WANG,<sup>1</sup> YICHENG WANG,<sup>1</sup> JIAN ZHANG,<sup>2</sup> PENG LIU,<sup>3</sup> XIAODONG XU,<sup>3</sup> YING LIU,<sup>3</sup> DEYUAN SHEN,<sup>3</sup> JI EUN BAE,<sup>4</sup> TAE GWAN PARK,<sup>4</sup> FABIAN ROTERMUND,<sup>4</sup> XAVIER MATEOS,<sup>5</sup> PAVEL LOIKO,<sup>6</sup> ZHENGPING WANG,<sup>7</sup> XINGGUANG XU,<sup>7</sup> JUN XU,<sup>8</sup> MARK MERO,<sup>1</sup> UWE GRIEBNER,<sup>1</sup> VALENTIN PETROV,<sup>1</sup> AND WEIDONG CHEN<sup>1,9,\*</sup>

<sup>1</sup>Max Born Institute for Nonlinear Optics and Short Pulse Spectroscopy, Max-Born-Str. 2a, D-12489 Berlin, Germany

<sup>2</sup>Key Laboratory of Transparent and Opto-Functional Inorganic Materials, Shanghai Institute of Ceramics, Chinese Academy of Sciences, Shanghai 201800, China

<sup>3</sup>Jiangsu Key Laboratory of Advanced Laser Materials and Devices, School of Physics and Electronic Engineering, Jiangsu Normal University, Xuzhou 221116, China

<sup>4</sup>Department of Physics, Korea Advanced Institute of Science and Technology (KAIST), 34141 Daejeon, Korea

<sup>5</sup>Física i Cristal·lografia de Materials i Nanomaterials (FICMA-FICNA), Universitat Rovira i Virgili (URV), Campus Sescelades, c/ Marcel·li Domingo, s/n., E-43007 Tarragona, Spain

<sup>6</sup>Centre de Recherche sur les Ions, les Matériaux et la Photonique (CIMAP), UMR 6252 CEA-CNRS-ENSICAEN, Université de Caen, 6 Boulevard du Maréchal Juin, 14050 Caen Cedex 4, France

<sup>7</sup>State Key Laboratory of Crystal Materials and Institute of Crystal Materials, Shandong University, Jinan 250100, China

<sup>8</sup>School of Physics Science and Engineering, Institute for Advanced Study, Tongji University, Shanghai 200092, China

<sup>9</sup>Key Laboratory of Optoelectronic Materials Chemistry and Physics, Fujian Institute of Research on the Structure of Matter, Chinese Academy of Sciences, Fuzhou, 350002, Fujian, China

\*Corresponding author: [chenweidong@fjirsm.ac.cn](mailto:chenweidong@fjirsm.ac.cn)

Received XX Month XXXX; revised XX Month, XXXX; accepted XX Month XXXX; posted XX Month XXXX (Doc. ID XXXXX); published XX Month XXXX

**Passive mode-locking of a Tm:LuYO<sub>3</sub> ceramic laser in the 2-μm spectral region is demonstrated by employing a SWCNT-SA. Almost chirp-free pulses as short as 57 fs, i.e., 8 optical cycles are produced at a repetition rate of 72.6 MHz (63 mW average power). The corresponding optical spectrum centered at 2045 nm, exhibits a bandwidth of 80 nm, which corresponds to almost chirp-free pulses. To the best of our knowledge, the results represent the shortest pulses generated by mode-locked Tm solid-state lasers.**

<http://dx.doi.org/10.1364/OL.99.099999>

Thulium (Tm<sup>3+</sup>) doped sesquioxide crystals are characterized by excellent thermo-optical and mechanical properties, relatively low maximum phonon energy and strong crystal fields. These features make them ideally suited for high power and broad-band tunable lasers in the 2-μm spectral region [1-4]. The strong crystal field splits the ground state of the Tm<sup>3+</sup> ion up to 800 cm<sup>-1</sup>, resulting in an emission bandwidth of more than 200 nm centered at 1950 nm [1]. Thus, the laser emission wavelength can easily be shifted to a

wavelength above 2 μm, hence supporting stable femtosecond pulse generation even without purging the laser cavity. Using Tm-doped sesquioxide crystals, 175-fs pulse generation has been reported for a Tm:Lu<sub>2</sub>O<sub>3</sub> laser mode-locked by a single-walled carbon nanotube (SWCNT) saturable absorber (SA) [5] and 166-fs pulses have been demonstrated for a Kerr-lens mode-locked Tm:Sc<sub>2</sub>O<sub>3</sub> laser [6]. Further shortening of the pulse duration was realized by using mixed sesquioxides as gain media, resulting in compositional disorder, which provides slightly broader and smoother gain spectra as compared to the ordered sesquioxide crystals [1, 7, 8].

One notable disadvantage of the cubic sesquioxide crystals is their high melting temperature which exceeds 2400 °C, underlying a high mechanical and chemical stability, however, presenting a challenge for the crystal growth [1]. In comparison, sesquioxide ceramics, as an alternative solution, can be fabricated at much lower temperatures and without phase transition. The investigated Tm:LuYO<sub>3</sub> mixed ceramic was sintered by Hot Isostatic Pressing (HIP) method at a lower temperature of 1700 °C [9]. In fact, the performance of sesquioxide ceramics used as gain media for mode-locking is comparable or even superior to single crystals, e. g., 180-fs pulses were generated from a Tm:Lu<sub>2</sub>O<sub>3</sub>

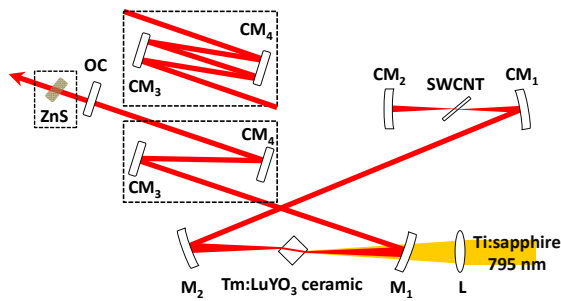


**Fig. 1.** Schematic of the SWCNT-SA mode-locked Tm:LuYO<sub>3</sub> ceramic laser. (L, lens; M<sub>1</sub>-M<sub>2</sub>, dichroic mirrors; CM<sub>1</sub>-CM<sub>4</sub>, chirped mirrors; OC, output coupler).

ceramic laser using semiconductor SA mirror (SESAM) for mode-locking [10], and pulses as short as 63 fs were reported recently employing a Tm:(Lu<sub>2/3</sub>Sc<sub>1/3</sub>)<sub>2</sub>O<sub>3</sub> mixed ceramic [11].

In this letter, mode-locking of a Tm:LuYO<sub>3</sub> mixed ceramic is demonstrated using a SWCNT-SA. After external dispersion management with a 3-mm-thick ZnS plate, pulses as short as 57 fs are achieved, i.e., 8 optical cycles estimated from the fringe-resolved interferometric autocorrelation.

The experimental setup of the SWCNT-SA mode-locked Tm:LuYO<sub>3</sub> ceramic laser is shown in Fig. 1. A standard X-shaped astigmatism compensated cavity was employed. The pump source was a continuous-wave (CW) Ti:sapphire laser tuned to 795 nm. Using a lens with a focal length of  $f = 70$  mm, the pump beam was focused into the ceramic resulting in a beam radius of 30  $\mu\text{m}$ . The mixed (Lu<sub>0.5</sub>Y<sub>0.5</sub>)<sub>2</sub>O<sub>3</sub> or LuYO<sub>3</sub> ceramic was doped with 3 at.% Tm<sup>3+</sup> ions. The uncoated sample had dimensions of 3  $\times$  3  $\times$  3 mm<sup>3</sup>. The ceramic was placed inside the cavity at Brewster's angle. The astigmatism was compensated by using two plano-concave mirrors, M<sub>1</sub> and M<sub>2</sub>, both with radius of curvature, RoC = -100 mm. The calculated beam radius at the position of the Tm:LuYO<sub>3</sub> ceramic were 30 and 60  $\mu\text{m}$  in the sagittal and tangential plane respectively. To mitigate the thermal load, the ceramic was wrapped with indium foil and tightly mounted in a copper holder which was water-cooled to 14.0  $^{\circ}\text{C}$ . The SWCNT-SA was deposited on a 1-mm-thick quartz substrate ( $\sim 1\%$  non-saturable loss,  $< 0.5\%$  modulation depth and  $< 10 \mu\text{J}/\text{cm}^2$  saturation fluence around 2  $\mu\text{m}$  [12]). It was placed in the second cavity waist under Brewster's angle, leading to beam radii of 70 and 105  $\mu\text{m}$  in the sagittal and tangential plane, respectively. The second cavity waist was formed by two concave chirped mirrors, CM<sub>1</sub> and CM<sub>2</sub>, with RoC = -100 and -50 mm respectively. Two further plane parallel chirped mirrors (CM<sub>3</sub> and CM<sub>4</sub>) with 2 or 4 beam bounces were employed to optimize the dispersion. The group delay dispersion (GDD) provided by each of them was  $-125 \text{ fs}^2$  per bounce. Three plane-wedged mirrors with transmission of 3%, 1.5% and 0.5% were used as output couplers (OCs). A 3-mm-thick ZnS polycrystalline (ceramic) with group velocity dispersion (GVD)  $\sim +155 \text{ fs}^2/\text{mm}$  at 2.05  $\mu\text{m}$  was employed for extracavity dispersion optimization. A commercial autocorrelator (pulseCheck, APE GmbH, Berlin, Germany) and a home-built second-harmonic generation (SHG) frequency-resolved optical gating (FROG) apparatus were used for temporal characterization of the output.

At first the CW wavelength tunability of the Tm:LuYO<sub>3</sub> ceramic laser was investigated by using a 3.2-mm-thick birefringent quartz plate (Lyot filter) in the cavity (without chirped mirrors and SWCNT-SA). The Tm:LuYO<sub>3</sub> ceramic pump absorption showed

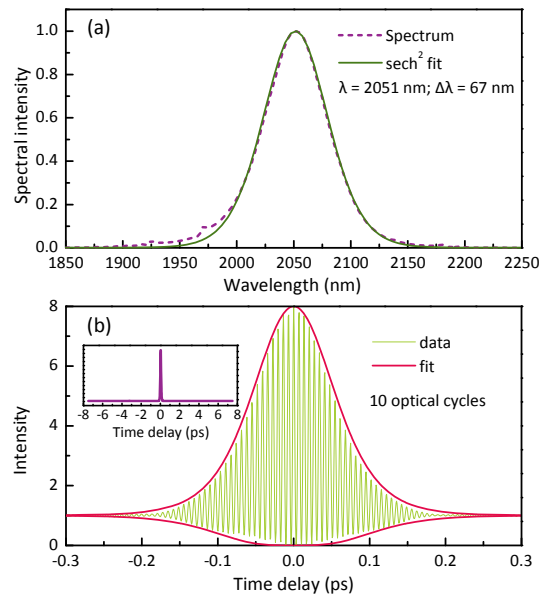


**Fig. 2.** Mode-locked Tm:LuYO<sub>3</sub> ceramic laser ( $T_{\text{OC}} = 3\%$ ). Optical spectrum (a) and interferometric autocorrelation trace (b). Inset (b): corresponding noncollinear autocorrelation trace on a time scale of  $\pm 7.5$  ps.

bleaching effects and depended on the specific OC used: e.g., it amounted to  $\square 63\%$  under lasing conditions with  $T_{\text{OC}} = 0.5\%$ . For this OC, the absorbed power at threshold was as low as  $\square 140$  mW. Using  $T_{\text{OC}} = 1.5\%$ , the laser was tunable from 1909 to 2109 nm. The maximum output power obtained with this output coupler amounted to 440 mW at 2074.2 nm, which coincided with the free-running wavelength in this case. This 200 nm CW tuning range exceeds the one reported for the Tm:(Lu<sub>2/3</sub>Sc<sub>1/3</sub>)<sub>2</sub>O<sub>3</sub> mixed ceramic laser of 130 nm, achieved under similar conditions [11].

For the mode-locking experiments, the SWCNT-SA was inserted in the cavity. The physical cavity length was extended by introducing the chirped mirrors, initially to  $\sim 1.75$  m using two beam bounces per round trip on each of the mirrors CM<sub>3</sub> and CM<sub>4</sub>. In this configuration the total round-trip GDD amounted to  $-1100 \text{ fs}^2$  taking into account also the material dispersion mainly due to the 1-mm-thick quartz substrate of the SA (GVD:  $-112 \text{ fs}^2/\text{mm}$  at 2050 nm). The contribution of the ceramic sample, estimated by averaging the corresponding refractive index data for Y<sub>2</sub>O<sub>3</sub> and Lu<sub>2</sub>O<sub>3</sub> crystals [13], was roughly  $+50 \text{ fs}^2$  per round trip and obviously negligible.

Mode locking of the Tm:LuYO<sub>3</sub> ceramic laser was self-starting for all output couplers applied. Using  $T_{\text{OC}} = 3\%$  an average output power of 210 mW was achieved for 2.1 W absorbed pump power. Taking into account the repetition rate of the laser, 85.6 MHz, the pulse energy amounts to  $\sim 2.5$  nJ. Thus the average pulse fluence on the SWCNT-SA was calculated to be  $\sim 350 \mu\text{J}/\text{cm}^2$ . Figure 2(a) shows the corresponding optical spectrum with a central wavelength at 2051 nm. The measured spectral profile can be fitted with a  $\text{sech}^2$ -function, giving a FWHM of 67 nm. The interferometric autocorrelation trace is shown in Fig. 2(b), assuming a  $\text{sech}^2$  pulse shape, yielding a pulse duration (FWHM) of 68 fs and a time-bandwidth product (TBP) of 0.325. The analysis of the autocorrelation trace envelopes indicates nearly chirp-free pulses [14] and counting the fringes one arrives at 10 optical cycles for the pulse duration. Single pulse operation without satellites

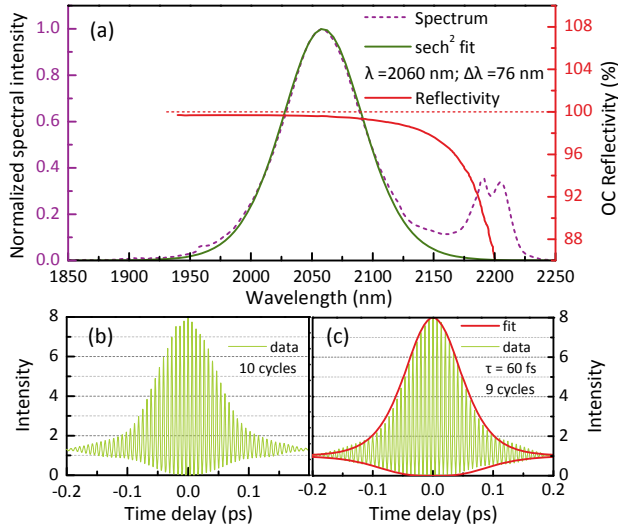


**Fig. 3.** Optical spectrum (a) of the mode-locked Tm:LuYO<sub>3</sub> ceramic laser with  $T_{oc} = 0.5\%$ , and the corresponding interferometric autocorrelation traces before (b) and after (c) compression. The red curve in (a) shows the reflectivity of the output coupler.

was confirmed by recording the noncollinear autocorrelation trace on a longer time scale of  $\pm 7.5$  ps, see the inset of Fig. 2(b). It should be noted that the on-axis intracavity laser intensity on the ceramic was estimated to be  $43 \text{ GW/cm}^2$ , which is comparable to the  $45 \text{ GW/cm}^2$  reported for the Kerr-lens mode-locked Tm:Sc<sub>2</sub>O<sub>3</sub> laser in [6], delivering 298-fs pulses. However, pure Kerr-lens mode-locking was not achieved in our laser configuration.

The present results seem of high importance for Ho-doped power amplifiers, mainly based on Ho:YLF or Ho:YAG [15] because the number of 2- $\mu\text{m}$  laser sources which meet the spectral requirements for seeding these amplifiers is very limited [16]. The center wavelength of the mode-locked Tm:LuYO<sub>3</sub> ceramic laser of 2051 nm exactly fits the gain maximum of Ho:YLF.

Subsequently, an OC with transmission of 0.5% was used in the mode-locked Tm:LuYO<sub>3</sub> mixed ceramic laser, delivering 70 mW average output power at 2 W of absorbed pump power. Compared to the laser with  $T_{oc} = 3\%$  the average pulse fluence on the SWCNT-SA increased to  $700 \mu\text{J/cm}^2$ . As shown in Fig. 3(a), the central emission wavelength was red-shifted to 2060 nm. This is attributed to the lower population inversion required thereby resulting in stronger reabsorption during the lasing process. As in the case of the operation with  $T_{oc} = 3\%$ , the spectral envelope was fitted well with a sech<sup>2</sup>-intensity profile except for the small peaks in the long-wave wing, which originated from the leakage of the 0.5% OC. (see its reflectivity curve in Fig. 3(a)). The pulse spectral FWHM amounted to 76 nm. The measured pulse duration using noncollinear autocorrelation amounted to 67 fs. In this case, the on-axis intracavity intensity on the ceramic reached  $86 \text{ GW/cm}^2$ , leading to a further spectral broadening due to a stronger self-phase modulation (SPM) compared to the  $T_{oc} = 3\%$  case. However, the increased TBP value of 0.36 indicated the existence of a residual pulse chirp. This chirp could be eliminated using the 3-mm-thick ZnS ceramic sample. Interferometric autocorrelation traces recorded without and with the ZnS sample are shown in Fig. 3(b) and 3(c), respectively. Obviously, the pulse duration was reduced to 60 fs, i.e., from 10 to 9 optical cycles. The fits to the optical spectrum and the envelopes of the interferometric

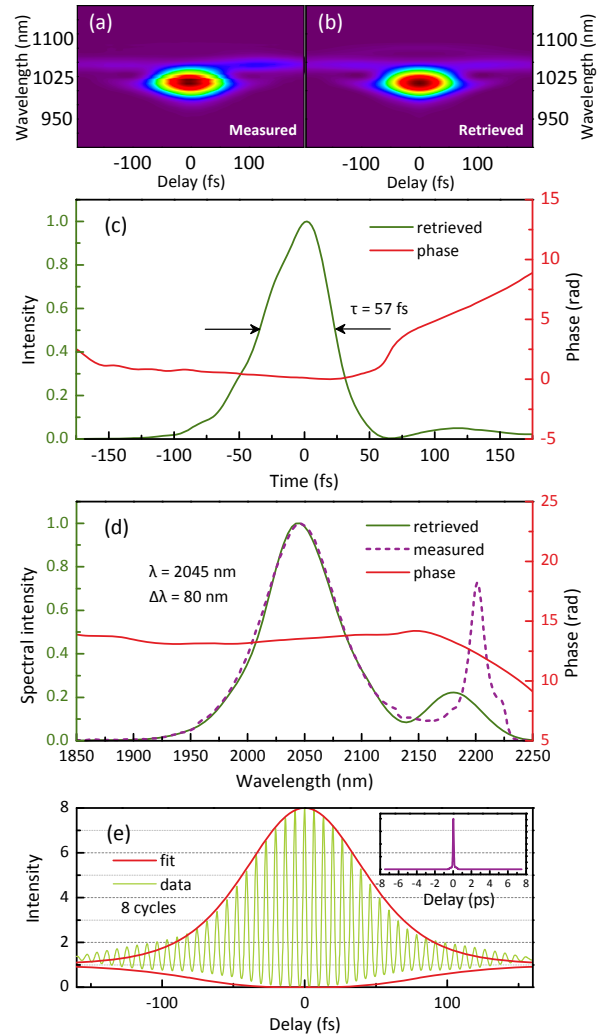


**Fig. 4.** Mode-locked Tm:LuYO<sub>3</sub> ceramic laser ( $T_{oc} = 0.5\%$ ) – shortest pulses. Measured (a) and retrieved (b) SHG-FROG traces after external pulse compression using ZnS, and the reconstructed temporal (c) and spectral (d) intensity and phase profiles; the dashed line in (d) is the measured optical spectrum. (e) interferometric autocorrelation trace. Inset (e): corresponding noncollinear autocorrelation trace on a time scale of  $\pm 7.5$  ps.

autocorrelation assuming a sech<sup>2</sup> pulse shape in Fig. 3, resulted in a TBP of 0.322.

The shortest pulses were generated by lengthening the cavity with the 0.5% OC up to  $\sim 2$  m in order to further increase the intracavity pulse energy. Despite the slight drop in the average output power down to 63 mW, the average intracavity fluence on the SWCNT-SA increased to  $\sim 750 \mu\text{J/cm}^2$ . The stronger SPM was balanced by increased GDD =  $-1600 \text{ fs}^2$  realized by four bounces per round trip on each of the mirrors CM<sub>3</sub> and CM<sub>4</sub>, see Fig. 1. The output pulses behind the ZnS plate were characterized by SHG-FROG.

Figures 4(a)–4(d) display the measured and reconstructed SHG-FROG traces together with the retrieved temporal and spectral profiles and phases. The FROG error between the measured and reconstructed SHG-FROG traces on a  $128 \times 128$  grid was 0.006. As shown in Fig. 4(c), the retrieved pulse duration amounted to 57 fs, corresponding to  $\sim 8$  optical cycles. From Fig. 4(d), it can be seen

that the reconstructed spectrum profile coincided well with the measured one, except for the already discussed sideband at longer wavelengths (see Fig. 3(a)). The center wavelength was at 2045 nm and the spectral FWHM amounted to 80 nm, giving a TBP of 0.327 which indicates almost transform-limited pulses. The residual chirp was deduced to be  $\pm 20 \text{ fs}^2$  by fitting the phase profile of the main spectral peak. At such a low chirp value, it was impossible to determine unambiguously the sign with the help of a substrate. The 8 optical cycles under the pulse envelope were confirmed by the recorded fringe-resolved interferometric autocorrelation trace (Fig. 4(e)). Single pulse operation without satellites was confirmed by a measurement on a longer time scale (inset in Fig. 4(e)). Since the pulses were almost chirp-free, the deviation from the fit based on a  $\text{sech}^2$ -intensity pulse shape was again attributed to the long-wavelength leakage of the 0.5% OC.

Note that the ZnS plate used outside the cavity in the present set-up operates only as a linear compression element which in fact helps to finely adjust the net intracavity GDD that can be controlled only in a stepwise manner by the chirped mirrors. The estimated nonlinear phase shift (B-integral) for the axial field does not exceed 0.2 mrad according to the nonlinear refractive index of ZnS near 2- $\mu\text{m}$  [17]. As expected for such small values, no difference in the output spectrum with and without the ZnS plate could be observed.

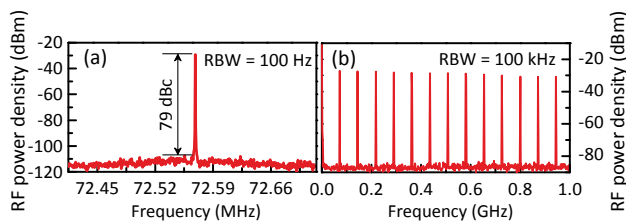


**Fig. 5.** Radio frequency spectra of the mode-locked Tm:LuYO<sub>3</sub> ceramic laser in 300 MHz (a) and 1 GHz (b) span range ( $T_{\text{OC}} = 0.5\%$ ).

To assess the stability of the SWCNT-SA mode-locked Tm:LuYO<sub>3</sub> ceramic laser, radio frequency (RF) spectra were recorded for the shortest pulses. Figure 5(a) shows the fundamental beat note at 72.57 MHz with an extinction ratio above the noise level of 79 dBc. This high contrast and the uniform harmonic beat notes in a wide span of 1 GHz (see Fig. 5(b)) indicate stable and CW mode-locked operation. All presented mode-locked Tm:LuYO<sub>3</sub> ceramic laser configurations run stable for hours.

In conclusion, we have demonstrated a SWCNT-SA mode-locked Tm:LuYO<sub>3</sub> ceramic laser generating sub-10-optical-cycle pulse in the 2- $\mu\text{m}$  spectral range. Its free-running laser wavelength above 2  $\mu\text{m}$  together with a 200 nm broad CW laser tuning range underline the excellent suitability of this novel Tm:LuYO<sub>3</sub> mixed ceramic for sub-100-fs pulse generation. In the mode-locked regime a maximum output power of 210 mW was achieved at 85.6 MHz repetition rate. In this case 68 fs pulses were generated with an optical spectrum centered at 2051 nm. Broadening of the spectral FWHM from 67 to 80 nm was achieved by increasing the intracavity power when using a low transmission of the OC ( $T_{\text{OC}} = 0.5\%$ ). Almost chirp-free pulses as short as 57 fs (TBP = 0.327) at 2045 nm, with an output power of 63 mW were achieved, corresponding to only 8 optical cycles, which to the best of our knowledge is the shortest pulse duration ever reported for a mode-locked Tm laser in the 2  $\mu\text{m}$  spectral range. Although pure

Kerr-lens mode locking was not observed with the present set-up, from estimations of Tm:Lu<sub>2</sub>O<sub>3</sub> ceramic at 2070 nm [10], the nonlinear refractive index shall be of the order of  $3.3 \times 10^{-16} \text{ cm}^2/\text{W}$ , i.e., rather close to the value for Ti:sapphire near 800 nm, and we expect such a regime to be more easily achievable with somewhat longer ceramic samples of Tm:LuYO<sub>3</sub>.

**Funding.** National Natural Science Foundation of China (61975208, 51761135115, 61850410533, 61575199, 61875199), Deutsche Forschungsgemeinschaft (PE 607/14-1), Jiangsu Science Foundation for Outstanding Young Scholars (SBK2019030177); National Research Foundation of Korea (2017R1A4A1015426); Foundation of the Government of the Russian Federation (074-U01).

**Acknowledgment.** Y. Zhao acknowledges financial support from the Alexander von Humboldt Foundation through a Humboldt fellowship, and the Qilu Young Scholars Program of Shandong University. This project has received funding from the European Union's Horizon 2020 research and innovation programme under grant agreement No. 654148 Laserlab-Europe.

**Disclosures:** The authors declare no conflicts of interest.

## References

1. C. Kränkel, IEEE J. Sel. Top. Quantum Electron. **21**, 1602013 (2015).
2. P. Loiko, P. Koopmann, X. Mateos, J. M. Serres, V. Jambunathan, A. Lucianetti, T. Mocek, M. Aguilo, F. Diaz, U. Griebner, V. Petrov, and C. Kränkel, IEEE J. Sel. Top. Quantum Electron. **24**, 1600713 (2018).
3. E. J. Saarinen, E. Vasileva, O. Antipov, J. P. Penttinen, M. Tavast, T. Leinonen, and O. G. Okhotnikov, Opt. Express **21**, 23844 (2013).
4. O. Antipov, A. Novikov, S. Larin, and I. Obionov, Opt. Lett. **41**, 2298 (2016).
5. A. Schmidt, P. Koopmann, G. Huber, P. Fuhrberg, S. Y. Choi, D. I. Yeom, F. Rotermund, V. Petrov, and U. Griebner, Opt. Express **20**, 5313 (2012).
6. M. Tokurakawa, E. Fujita, and C. Kränkel, Opt. Lett. **42**, 3185 (2017).
7. A. A. Lagatsky, P. Koopmann, O. L. Antipov, C. T. A. Brown, G. Huber, and W. Sibbett, Conference on Lasers & Electro-Optics Europe CLEO EUROPE, Munich, 2013, OSA, paper CA\_6\_3.
8. N. K. Stevenson, C. T. A. Brown, J. M. Hopkins, M. D. Dawson, C. Kränkel, and A. A. Lagatsky, Opt. Lett. **43**, 1287 (2018).
9. Z. Y. Zhou, X. F. Guan, X. X. Huang, B. Xu, H. Y. Xu, Z. P. Cai, X. D. Xu, P. Liu, D. Z. Li, J. Zhang, and J. Xu, Opt. Lett. **42**, 3781 (2017).
10. A. A. Lagatsky, O. L. Antipov, and W. Sibbett, Opt. Express **20**, 19349 (2012).
11. Y. C. Wang, W. Jing, P. Loiko, Y. G. Zhao, H. Huang, X. Mateos, S. Suomalainen, A. Harkonen, M. Guina, U. Griebner, and V. Petrov, Opt. Express **26**, 10299 (2018).
12. W. B. Cho, J. H. Yim, S. Y. Choi, S. Lee, A. Schmidt, G. Steinmeyer, U. Griebner, V. Petrov, D. I. Yeom, K. Kim, and F. Rotermund, Adv. Funct. Mater. **20**, 1937 (2010).
13. D. E. Zelmon, J. M. Northridge, N. D. Haynes, D. Perlov, and K. Petermann, Appl. Opt. **52**, 3824 (2013).
14. J.-C. M. Diels, J. J. Fontaine, I. C. McMichael, and F. Simoni, Appl. Opt. **24**, 1270 (1985).
15. L. von Grafenstein, M. Bock, U. Griebner, and T. Elsaesser, Opt. Express **23**, 14744 (2015).
16. M. Hinkelmann, D. Wandt, U. Morgner, J. Neumann, and D. Kracht, Opt. Express **25**, 20522 (2017).
17. S. Vasilyev, I. Moskalev, M. Mirov, V. Smolski, S. Mirov, and V. Gapontsev, Opt. Mater. Express **7**, 2636 (2017).

## References

1. C. Kränkel, "Rare-Earth-Doped Sesquioxides for Diode-Pumped High-Power Lasers in the 1-, 2-, and 3- $\mu\text{m}$  Spectral Range," *IEEE Journal of Selected Topics Quantum Electronics* **21**, 1602013 (2015).
2. P. Loiko, P. Koopmann, X. Mateos, J. M. Serres, V. Jambunathan, A. Lucianetti, T. Mocek, M. Aguilo, F. Diaz, U. Griebner, V. Petrov, and C. Kränkel, "Highly Efficient, Compact  $\text{Tm}^{3+}:\text{RE}_2\text{O}_3$  (RE = Y, Lu, Sc) Sesquioxide Lasers Based on Thermal Guiding," *IEEE Journal of Selected Topics Quantum Electronics* **24**, 1600713 (2018).
3. E. J. Saarinen, E. Vasileva, O. Antipov, J. P. Penttinen, M. Tavast, T. Leinonen, and O. G. Okhotnikov, "2- $\mu\text{m}$   $\text{Tm}:\text{Lu}_2\text{O}_3$  ceramic disk laser intracavity-pumped by a semiconductor disk laser," *Optics Express* **21**, 23844 (2013).
4. O. Antipov, A. Novikov, S. Larin, and I. Obronov, "Highly efficient 2  $\mu\text{m}$  CW and Q-switched  $\text{Tm}^{3+}:\text{Lu}_2\text{O}_3$  ceramics lasers in-band pumped by a Raman-shifted erbium fiber laser at 1670 nm," *Optics Letters* **41**, 2298 (2016).
5. A. Schmidt, P. Koopmann, G. Huber, P. Fuhrberg, S. Y. Choi, D. I. Yeom, F. Rotermund, V. Petrov, and U. Griebner, "175 fs  $\text{Tm}:\text{Lu}_2\text{O}_3$  laser at 2.07  $\mu\text{m}$  mode-locked using single-walled carbon nanotubes," *Optics Express* **20**, 5313 (2012).
6. M. Tokurakawa, E. Fujita, and C. Kränkel, "Kerr-lens mode-locked  $\text{Tm}^{3+}:\text{Sc}_2\text{O}_3$  single-crystal laser in-band pumped by an Er:Yb fiber MOPA at 1611 nm," *Optics Letters* **42**, 3185 (2017).
7. A. A. Lagatsky, P. Koopmann, O. L. Antipov, C. T. A. Brown, G. Huber, and W. Sibbett, "Femtosecond pulse generation with Tm-doped sesquioxides," *Conference on Lasers & Electro-Optics Europe CLEO EUROPE, Munich, 2013*, OSA, paper CA\_6\_3.
8. N. K. Stevenson, C. T. A. Brown, J. M. Hopkins, M. D. Dawson, C. Kränkel, and A. A. Lagatsky, "Diode-pumped femtosecond  $\text{Tm}^{3+}$ -doped  $\text{LuScO}_3$  laser near 2.1  $\mu\text{m}$ ," *Optics Letters* **43**, 1287 (2018).
9. Z. Y. Zhou, X. F. Guan, X. X. Huang, B. Xu, H. Y. Xu, Z. P. Cai, X. D. Xu, P. Liu, D. Z. Li, J. Zhang, and J. Xu, " $\text{Tm}^{3+}$ -doped  $\text{LuYO}_3$  mixed sesquioxide ceramic laser: effective 2.05  $\mu\text{m}$  source operating in continuous-wave and passive Q-switching regimes," *Optics Letters* **42**, 3781 (2017).
10. A. A. Lagatsky, O. L. Antipov, and W. Sibbett, "Broadly tunable femtosecond  $\text{Tm}:\text{Lu}_2\text{O}_3$  ceramic laser operating around 2070 nm," *Optics Express* **20**, 19349 (2012).
11. Y. C. Wang, W. Jing, P. Loiko, Y. G. Zhao, H. Huang, X. Mateos, S. Suomalainen, A. Harkonen, M. Guina, U. Griebner, and V. Petrov, "Sub-10 optical-cycle passively mode-locked  $\text{Tm}:(\text{Lu}_{2/3}\text{Sc}_{1/3})_2\text{O}_3$  ceramic laser at 2  $\mu\text{m}$ ," *Optics Express* **26**, 10299 (2018).
12. W. B. Cho, J. H. Yim, S. Y. Choi, S. Lee, A. Schmidt, G. Steinmeyer, U. Griebner, V. Petrov, D. I. Yeom, K. Kim, and F. Rotermund, "Boosting the Nonlinear Optical Response of Carbon Nanotube Saturable Absorbers for Broadband Mode-Locking of Bulk Lasers," *Advanced Functional Materials* **20**, 1937 (2010).
13. D. E. Zelmon, J. M. Northridge, N. D. Haynes, D. Perlov, and K. Petermann, "Temperature-dependent Sellmeier equations for rare-earth sesquioxides," *Applied Optics* **52**, 3824-3828 (2013).
14. J.-C. M. Diels, J. J. Fontaine, I. C. McMichael, and F. Simoni, "Control and Measurement of Ultrashort Pulse Shapes (in Amplitude and Phase) with Femtosecond Accuracy," *Applied Optics* **24**, 1270 (1985).
15. L. von Grafenstein, M. Bock, U. Griebner, and T. Elsaesser, "High-energy multi-kilohertz Ho-doped regenerative amplifiers around 2  $\mu\text{m}$ ," *Optics Express* **23**, 14744 (2015).
16. M. Hinkelmann, D. Wandt, U. Morgner, J. Neumann, and D. Kracht, "Mode-locked Ho-doped laser with subsequent diode-pumped amplifier in an all-fiber design operating at 2052 nm," *Optics Express* **25**, 20522 (2017).
17. S. Vasilyev, I. Moskalev, M. Mirov, V. Smolski, S. Mirov, and V. Gapontsev, "Ultrafast middle-IR lasers and amplifiers based on polycrystalline Cr:ZnS and Cr:ZnSe," *Optical Materials Express* **7**, 2636-2650 (2017).